Optical and Quantum Electronics manuscript No.
(will be inserted by the editor)

Closed-loop Modeling of Silicon Nanophotonics

From Design to Fabrication and Back Again

Wim Bogaerts · Paul Bradt · Lieven Vanholme · Peter Bienstman · Roel Baets

Received: date / Accepted: date

Abstract We present a method for component-centric modeling of silicon nanophotonics, where a closed optimization loop allows to take the effects of the fabrication process into account during the design of nanophotonic components. This enables black-box component descriptions with functional parameters. Underlying mask layouts of the components can then automatically be optimized for their actual performance, and not just for their geometric layout. To simulate the effect of fabrication, we developed a projection lithography simulator which was included inside the optimization loop. This method was applied to the design of a 1-dimensional distributed Bragg mirror.

Keywords Modeling · Nanophotonics · Lithography · Design

1 Introduction

Nanophotonics in general, and especially silicon nanophotonics, allow the large-scale integration of submicron waveguides onto a photonic chip [Bogaerts(2005)]. However, the submicron dimension also make the waveguide components extremely sensitive to variations. This is relevant when implementing wavelength-selective functions [Bogaerts(2006)] such as ring resonators or interferometers, or nonlinear functions where the power distribution in the waveguide is important [Dumon(2006)]. In most cases, the imperfections are introduced during the fabrication stage, resulting in a mismatch between the originally designed (and modeled) device and the actual device. This is especially true when the fabrication process includes steps with a strong physical resolution limit, such as optical lithography.

W. Bogaerts acknowledges the Flemish Fund for Scientific Research (FWO) for a postdoctoral grant. Part of this work was funded by the European Union in the framework of the IST network of Excellence ePIXnet and the FP7 integrated project HELIOS. Part of this work was supported by the Belgian Science Policy through the IAP VI-10 project photonics@be

Ghent University - IMEC, Department of Information Technology
Sint-Pietersnieuwstraat 41
Tel.: +32-9-2643324
Fax: ++32-9-2643593
E-mail: wim.bogaerts@intec.ugent.be

In a typical photonic design flow, fabrication is not taken into account at all, except after the fact by comparing the characterization results with the original simulation and resimulating the device with the actual fabricated geometry. This can be fine for research, but it hardly allows for *first-time-right* designs.

In state-of-the-art electronics, the fabrication process is taken into account, albeit in a more limited way than we propose here. Typically, electronics is designed from a functional point of view, using behavioral models of electronic circuit blocks. When the correct circuit is designed, (automatic) placement and layout is done. Only then, after laying out the actual mask design, corrections to compensate for fabrication are added, to make the fabricated design resemble the original mask layout as closely as possible. Most electronic elements are designed in a sufficiently robust way that a geometric approximation will guarantee the correct functionality. This is not true in nanophotonics, where nanometer-scale variations can have serious impact.

The solution to this problem is to include the actual fabrication process into the design flow. This, of course, requires an accurate numerical model of the fabrication process, that can extract the correct component geometry from the layout that will be sent to the manufacturer (in the case of optical lithography: the mask shop). In this paper we elaborated this method, and we introduced a simulator for optical projection lithography between the mask layout and the electromagnetic simulation of the component. This design procedure was then fitted into an optimization algorithm which converged to the optimal mask layout.

In the next section we will describe the problem in more detail. In section 3 we discuss the design method in more detail and describe our implementation. Section 4 describes the lithographic simulation tool we developed for the virtual fabrication. Finally, in section 5 we apply the tool to an example, in this case a distributed Bragg mirror embedded into a photonic wire waveguide.

2 The problem of nanophotonic design

It is very difficult to make nanophotonic components exactly as one has designed them. Because of the submicron features, most people employ e-beam lithography [Vlasov(2004)]. This technique is slow and unsuitable for mass-fabrication, but has a very high resolution. Even then, it is still difficult to fabricate nanophotonic components on target. With optical lithography, this problem is worse.

2.1 Accuracy

In high-contrast waveguides and filters, the spectral accuracy, i.e. the accuracy with which a particular wavelength-dependent behavior can be implemented, is extremely sensitive to the actual geometry. Typically, a change in critical dimension (CD) of $1nm$ results in a wavelength shift of the same order of magnitude. This CD can be the waveguide width, but also the length of a low-order cavity or the hole diameter in a photonic crystal.

While it is impossible to eliminate all variation in CD, it is important to keep them as small as possible. In many cases, small deviations from the actual design can be compensated by low-power thermal tuning. The larger the deviation, the higher the

tuning power that is needed, and in some components with complex behavior, simple tuning cannot compensate for the change in layout.

In photonic circuits, many different patterns are printed together in the same layer. For example, a photonic wire is an isolated line, while a photonic crystal is a dense array of holes. These different features have different optimum exposure conditions, especially a different exposure dose-to-target. In addition, as the feature size and pitch goes down to the resolution limit, the pattern definition becomes less accurate. This is most obvious in rounding of corners and shortening of narrow lines. But more subtle are optical proximity effects: the image after lithography depends very strongly on the density of the mask features and their immediate environment. An isolated line will print differently when another line is nearby (typically within $1\,\mu m$), and photonic crystal holes at the edge of a lattice will differ from the holes in the bulk [Bogaerts(2002)].

Because of this extreme sensitivity to deviations introduced during fabrication, the fabrication process should be included in the design method, allowing to optimize the design as it is fabricated, and not as it is laid out on the photomask. Lithographic deviation from the mask layout are mostly deterministic, and can be modeled, as is discussed in the section 4. Other deviations are statistical in nature, such as sidewall roughness and wafer layer thickness. These are more difficult to predict, and so in the end, a tuning mechanism is still required for most functions.

2.2 A cumbersome design cycle

Another problem with nanophotonic design is that many people use a fragmented tool set, which are used in a disjunct way. First, a photonic component is geometrically defined for electromagnetic simulation. If needed, the geometry is optimized until the behavior is acceptable. Then, a mask layout is drawn, most likely in another tool, that matches the simulated structure. In some cases, post-layout proximity corrections could be added. Many steps (like the geometric definition) have to be repeated, making the whole process prone to human errors. Also, this design cycle takes the fabrication into account only at the last step. And these correction are often not sufficient to compensate for the deviations introduced by the fabrication.

3 Component-centric design

3.1 Concept

To facilitate the design process, we decided to implement a component-centric design for photonics. In most electronics design libraries, building blocks are implemented as self-contained entities which can generate their mask layout, as well as provide a behavioral model. A similar approach for photonics is also desirable. Only, behavioral models for nanophotonic components (especially when they are parametric) often require calculations down to the physical electromagnetic simulations.

This means that for component-centric design to work in photonics, an accurate virtual fabrication, and subsequent electromagnetic modeling tool is required. The actual fabrication parameters are then supplied by the user or the foundry through a separate technology description (e.g. *tech* files), not unlike in electronics. This concept is shown in figure 1a.

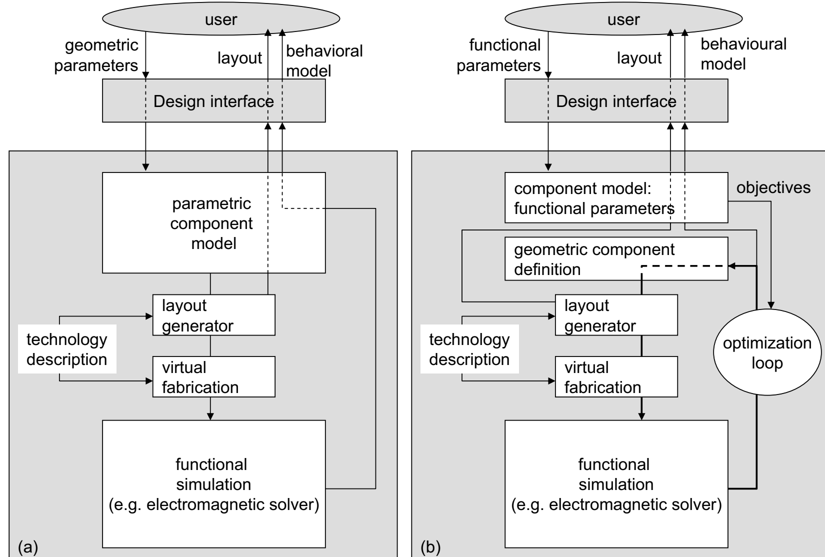

Fig. 1 A component-centric design process. (a) with geometric parameters; (b) with behavioral parameters.

In this model, we can extract the behavior of a component when supplying the geometric parameters of the mask layout, including optical proximity correction (OPC) features. However, it is possible to make further abstraction of the component. Instead of geometric parameters (which implies some knowledge of the layout of the component), we could supply functional parameters to the component, without knowing anything about the actual layout of the component. E.g. a wavelength filter could be implemented as a ring resonator cascade, or as a lattice filter of Mach-Zehnder interferometers [Bogaerts(2006)]; the user would only supply some parameters of the filter characteristic.

Such an abstraction places a strong demand on the underlying component model. To obtain the demanded behavior, the geometric layout of the component should be chosen to result in the desired behavior after fabrication. This is a complex problem which is difficult to solve directly. Hence, a behind-the-scene optimization loop is required to match the actual behavior with the desired behavior and determine the exact component layout. This is shown in figure 1b. Of course, for the functional behaviour to be modeled directly, a geometric layout is required. However, this could be kept hidden from the user, effectively supplying a functional black box.

3.2 Implementation

We have implemented a proof of concept for this design with hierarchical simulation. *Python* was used as the core language [Bienstman(2007)], as it is extremely easy to use as an interface language to many libraries. We employed the following tools to handle the different aspects of the design cycle:

- A large set of parametric mask layouts for photonic component are described in the *PICAZZO* library, developed at Ghent University - IMEC.
- *IPKISS* is a python library that can generate mask layouts for *PICAZZO* in various file formats.
- To simulate the fabrication, we developed a lithography simulator in-house, which is described in section 4. However, an interface to any other (commercial) lithography simulator could be used [Mack(1985),Fühner(2007)].
- The electromagnetic simulation of the virtually fabricated device was done using the eigenmode expansion solver *CAMFR* [Bienstman(2001)].
- The optimization loop was governed by an informed particle swarm optimization algorithm [Mendes(2004)].

4 Optical Projection Lithography Simulation

As the most limiting factor in our fabrication process is the optical lithography, we decided to use a lithography simulator for our virtual fabrication step. In optical projection lithography, the patterns from a (transmissive) mask are projected onto a photosensitive resist through a lens system. These projection systems consist of complex lens combinations, but they typically adhere to a so-called Kohler setup, shown in figure 2 where the pupil (the element constraining the numerical aperture of the system) of the entire lens system is located in the fourier plane of the mask image [Mack(2006), Levinson(2001)]. This allows us to make abstraction of the lens system and the source and approximate the entire projection process using Fourier optics [Kintner(1978)]. This includes an extended source, or even off-axis illumination. An extended source is specified by its size σ, which is its size in the pupil plane relative tot the size of the entire pupil.

In this model, the lowest periodicity or pitch Λ of structures that can be imaged is given by

$$\Lambda_{min} = \frac{\lambda}{NA\,(1+\sigma)}, \tag{1}$$

with λ the illumination wavelength and NA the numerical aperture of the lens system (directly proportional to the size of the pupil)[Levinson(2001)]. This is a theoretical limit, as near the resolution limit the image contrast will be very low. For our experiments we used $248\,nm$ lithography [Bogaerts(2005)], but recently we switched to an ASML PAS5500/1100, with an illumination at $193\,nm$ for higher resolution [Selvaraja(2008)]. With this tool, depending on the actual exposure parameters, it is possible to print dense features with a pitch down to about $260\,nm$.

While a number of commercial lithography simulation tools exist, we chose to write a simple, but fast model which could easily be coupled to our design tools. The model was also developed in the language *Python*, using the *Numpy* extensions for matrix calculations [Bienstman(2007)]. The following calculation steps are followed:

- First, a partially coherent modulation transfer function (MTF) of the optical system is calculated from the wavelength, numerical aperture and the shape of the extended source [Kintner(1978)]. The MTF is only calculated for the relevant spatial frequencies and the result is cached for later use.
- The mask image is Fourier transformed and multiplied with the MTF. The result is transformed back to obtain the image intensities in the photoresist.

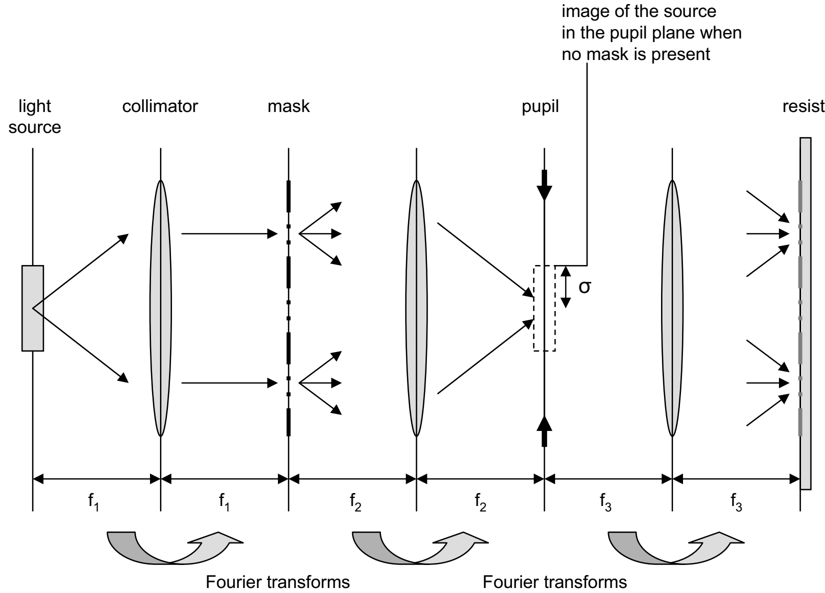

Fig. 2 Kohler setup for optical projection lithography.

- From a simple resist model (either a straightforward threshold model or a Dill model) the resist pattern on the wafer is extracted. In our case, the resist model was calibrated against actual fabrication data.
- Finally, in a simple approximation, we assume the resist pattern is transferred without distortion into the silicon material.

In addition to extended sources, the model can also include defocus and lens aberrations. Still, our lithographic model makes a number of approximations, making it less accurate than other (commercial) tools. The main limitation is the use of Fourier optics, which makes it less suitable for high-NA lens systems. For instance, it does not (yet) take into account polarization effects or a finite resist thickness. However, it is quite efficient, and calibration against actual fabricated devices show that the model is already sufficiently accurate for all but the smallest features. We are currently in the process of fabricating test structures to further calibrate this model. Still, when going for maximum accuracy, it is always possible to replace it in the simulation cycle with a high-end commercial tool [Mack(1985),Fühner(2007)].

Also, for the lithographic simulations we made use of the mask layout, ignoring possible imperfections in the photomask. As photomasks are written by e-beam lithography at a magnification of 4X, the imperfections will be small compared to the effects of the optical lithography, but when scaling down to ever smaller features the photomask could start playing a significant role.

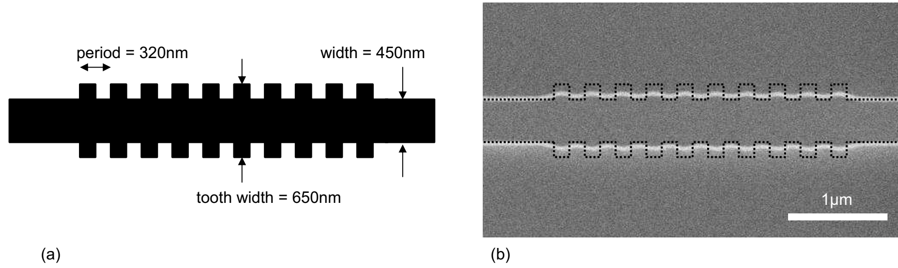

Fig. 3 Distributed Bragg mirror in a photonic wire. (a) Original mask design, (b) fabricated device.

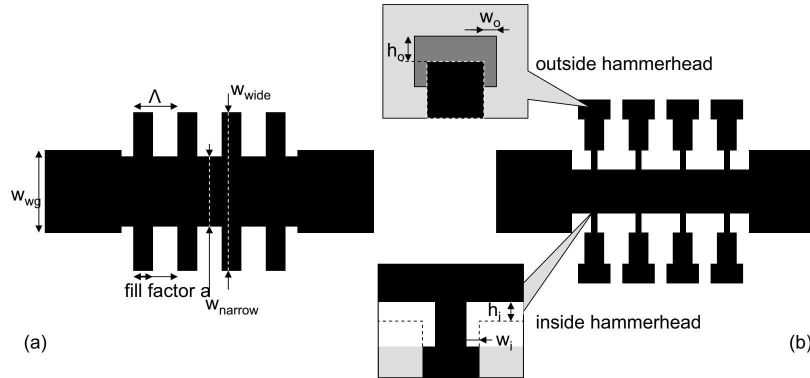

Fig. 4 Geometric parameters for a parametric DBR component in the PICAZZO library. (a) Simple DBR, (b) DBR with hammerhead OPC features.

5 Example: a 1-D distributed Bragg mirror

5.1 Problem description

As an example, we used the tools in section 3 to optimize a distributed Bragg reflector (DBR) embedded in a photonic wire [Gnan(2004),Gnan(2006)]. For good reflection, we want to implement a compact first-order grating for a wavelength around $1.55\,\mu m$. However, in a silicon wire, this requires a grating pitch around $300\,nm$, very close to the resolution limit of our optical lithography process. Because of this, severe corner rounding will distort the DBR, resulting in a completely different reflection spectrum. An actual fabricated device is compared to its original mask layout in figure 3.

To get the desired functionality of this component, we have redesigned it using the component-centric design described in section 3. For this, we used 2 different parametric components with a geometric description of a 1-D DBR in a photonic wire. The components, together with their layout parameters are shown in figure 4. One is the DBR as it was originally conceived, with periodic lateral wings. In the second version, primitive optical proximity corrections (OPC) in the form of hammerheads are added. These should somewhat counteract the corner rounding in the device in figure 3.

However, we do not intend to control the geometric parameters directly. Instead, we supply a single functional parameter: the wavelength for which we want a strong

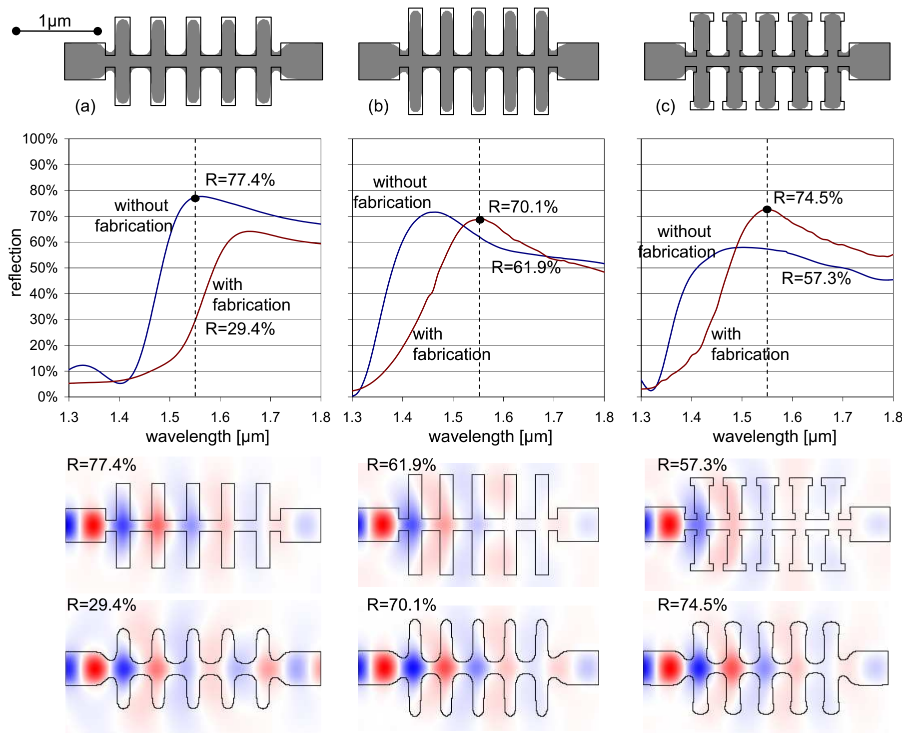

Fig. 5 Results from optimized DBR designs. Top to bottom: the design before and after virtual fabrication, reflection as a function of wavelength, and field plots at the target wavelength of $1.55\,\mu m$ with and without virtual fabrication. (a) Grating design from fig 4a optimized without taking the fabrication into account. (b) The same grating design, but optimized including the fabrication process and (c) the grating design with hammerhead from fig 4b optimized with virtual fabrication.

reflection. We will then leave it to the optimization algorithm to come up with the geometric parameters that give us the best reflection.

5.2 Modeling Results

The results of this optimization procedure are shown in figure 5. We optimized a DBR grating without hammerheads for a high reflectivity at a wavelength of $1550\,nm$. We did three optimizations. One where the virtual fabrication was not taken into the optimization loop, one where it was, and a final one where we added hammerhead OPC to correct for corner rounding. The results of these optimizations are shown in figure 5, and the exact design dimensions are listed in table 1. It shows the mask design that comes out of the optimization overlaid on the (virtually) fabricated component. The reflection of the devices as a function of wavelength is also plotted. Note that these full spectra were not calculated in the course of the optimization, but only afterwards to evaluate the effectiveness of the optimization. The objective function tried to maximize the reflection only at the target wavelength, also indicated in the figure.

Table 1 Geometric parameters after optimization for the three DBR gratings in figure 5

Parameter	(a)	(b)	(c)
pitch Λ [μm]	0.430	0.385	0.400
fill factor a	40%	42%	46%
wide width w_{wide} [μm]	1.070	1.300	1.085
narrow width w_{narrow} [μm]	0.150	0.150	0.205
hammerhead w_o [μm]			0.050
hammerhead h_o [μm]			0.055
hammerhead w_i [μm]			0.025
hammerhead h_i [μm]			0.030
Reflection			
without fabrication	**77.4%**	61.9%	57.3%
with fabrication	29.4%	**70.1%**	**74.5%**

For the design where fabrication was not included in the optimization, we see that the end result is a very poor transmission at the target wavelength after fabrication, with a strong shift of the reflection spectrum to longer wavelengths. In the end, the optimized reflection of 77.4% is reduced down to only 29.4%. For the DBR where the fabrication was taken into the loop, we find the opposite effect. The fabricated structure has a reflection of 70.1%, while the original mask layout performs worse, at 61.9%. Still, the optimized result is lower than what we got for the original optimization without using any virtual fabrication. In a third simulation, we try to improve this result by adding the hammerhead OPC features from figure 4b. Again, we take the fabrication into the optimization loop, and we end up with a reflection of 74.5%, which is a significant improvement to the design without OPC features. As we can see, the nature of optical lithography results in a very accurate reproduction of the designed periods, but with severe corner rounding and line-end shortening. The hammerheads alleviate both effects, and we see therefore that between designs (b) and (c) the length of the grating fins can be shortened somewhat.

The additional increase of the reflectivity due to the hammerheads can be attributed to the small size of the DBR grating (only 5 periods) and a mismatch between the incident waveguide mode and the grating. This results in unwanted scattering, and not the desired back reflection. This problem could be remedied by apodizing the first periods of the grating, and therefore taking the dimensions of the first periods in the optimization loop as separate variables.

In this example we used a simple objective function (maximize reflection at a single wavelength), but it is obvious that more complex objective functions could be defined such as reflections at multiple wavelengths or over a wavelength band, or maximizing reflection at one wavelength and transmission at another. This might have an impact on the simulation time. Simulations were done on a single processor. Without lithography simulation, the entire optimization cycle took 15 minutes (for simulating approximately 1000 variations of the DBR). With the lithography simulation includes, the simulation time increased to 3 hours. This is attributed to two aspects: The overhead of calculating the lithography, which amounts for approximately 45 minutes, and the fact that the resulting structures were much more irregular, and therefore more difficult to simulate with the CAMFR eigenmode expansion tool. The use of another technique, such as FDTD, would not induce the same penalty. This is possible, as the cycle is in no way

linked to the specific optimization algorithm we used here (particle swarm), or the electromagnetic simulation tool (CAMFR eigenmode expansion).

The drawback of using a stochastic optimization routine is that we cannot be sure to have reached the global optimum, as the objective function of the design can have multiple local optima.

6 Limitations and Perspectives

The modeling concept described above has a strong potential. However, it has some limitations as well. The requirement of physical modeling can be a performance killer for larger components. Using specific models for such components, or subcomponents can alleviate this. Also, smart caching algorithms can be used to store commonly used components, or the physical simulations could be offloaded to a heavy simulation cluster or supercomputer.

This strategy of integrating the fabrication process deeply into the design process is also done more frequently for high-end electronics manufacturing on the $45\,nm$ node and smaller. Here, the physical effects of small deviations due to fabrication begin the play a significant role. This method is often referred to as *technology aware design*.

In the future, component libraries will be provided by photonic foundries, just as it is in the electronics world. Here, too, the behavioral model for the standard components will be provides, but it is likely that these will be approximated in some analytical expression for performance, after having been thoroughly simulated or extracted from the fabricated structure. Still, for parametric components where the user can modify the geometric or functional description of the component, on-the-fly full electromagnetic simulations might be the only reliable way to come to a first-time-right design.

Both the predefined models as the directly simulated components are needed to enable circuit-level simulation of photonic components. e.g. for passive circuits, an S-matrix could be calculated for each component, which can then be fed to a circuit simulator [Leijtens(1996)Leijtens, LeLourec, and Smit]. For active components, a time-based circuit model can be used. For efficiency, such circuit models of individual components can be cached for later use. If the component is part of a (commercial) design kit, it is even possible to fit an analytical parametric model to the component based on a large number of electromagnetic simulations which are done in advance by the design kit builder.

Simply applying post-layout proximity corrections is not sufficient for nanophotonic components. Even with proximity corrections, one cannot obtain perfectly sharp corners. Therefore, the fabrication should be taken into the optimization loop.

7 Conclusion

We demonstrated the power of a component-centric design approach by implementing a behavioral model which, in the background, automatically converts a geometric mask layout into an electromagnetic response of the component. To take into account the effects of fabrication, we also developed an optical lithography simulator which we included in the optimization loop. This way, a functional parametric description of a component can be used at the design stage.

We demonstrated this technique on a 1-D distributed Bragg reflector embedded in a photonic wire waveguide. This structure is very representative, as its geometric features are close to the lithographic limit. This shows that the inclusion of the lithographic simulator into the design process is essential to design reliable nanophotonic components and circuits.

References

[Bienstman(2001)] Bienstman P, Baets R (2001) Optical modelling of photonic crystals and vcsels using eigenmode expansion and perfectly matched layers. Opt Quantum Electron 33(4/5):327

[Bienstman(2007)] Bienstman P, Vanholme L, Bogaerts W, Dumon P, Vandersteegen P (2007) Python in nanophotonics research. Comp. Science Eng 9(3):2801–2803

[Bogaerts(2002)] Bogaerts W, Wiaux V, Taillaert D, Beckx S, Luyssaert B, Bienstman P, Baets R (2002) Fabrication of photonic crystals in Silicon-on-insulator using 248-nm deep UV lithography. IEEE J Sel Top Quantum Electron 8(4):928–934

[Bogaerts(2005)] Bogaerts W, Baets R, Dumon P, Wiaux V, Beckx S, Taillaert D, Luyssaert B, Van Campenhout J, Bienstman P, Van Thourhout D (2005) Nanophotonic waveguides in Silicon-on-insulator fabricated with CMOS technology. J Lightwave Technol 23(1):401–412

[Bogaerts(2006)] Bogaerts W, Dumon P, Van Thourhout D, Taillaert D, Jaenen P, Wouters J, S B, Wiaux V, Baets R (2006) Compact wavelength-selective functions in silicon-on-insulator photonic wires. J Sel Top Quantum Electron 12(6):1394–1401

[Dumon(2006)] Dumon P, Priem G, Nunes L, Bogaerts W, Van Thourhout D, Bienstman P, Liang T, Tsuchiya M, Jaenen P, Beckx S, Wouters J, Baets R (2006) Linear and nonlinear nanophotonic devices based on silicon-on-insulator wire waveguides. Jap. J. Appl. Phys. 1 45(8B):6589–6602

[Fühner(2007)] Fühner T, Schnattinger T, Ardelean G, Erdmann A (2007) Dr.litho: a development and research lithography simulator. Proc. SPIE Microlithography 6520, p 65203F,

[Gnan(2004)] Gnan M, Chong H, Kim C, Bryce A, Sorel M, De La Rue R (2004) Coupled microcavity in photonic wire bragg grating. Lasers and Electro-Optics, 2004 (CLEO) Conference on 1:2 pp. vol.1–,

[Gnan(2006)] Gnan M, Bellanca G, Chong H, Bassi P, Rue R (2006) Modelling of photonic wire Bragg gratings. Opt. Quantum Electron 38(1-3):133–148

[Kintner(1978)] Kintner E (1978) Method for the calculation of partially coherent imagery. Appl Opt 17(17):2747–2753

[Leijtens(1996)Leijtens, LeLourec, and Smit] Leijtens X, LeLourec P, Smit M (1996) S-matrix oriented CAD-tool for simulating complex integrated optical circuits. J. Sel. Top. Quantum Electron. 2(2):257–262

[Levinson(2001)] Levinson HJ (2001) Principles of Lithography. SPIE, Bellingham, Washington, USA

[Mack(1985)] Mack C (1985) Prolith - a Comprehensive Optical Lithography Model. Proc SPIE 538:207–220

[Mack(2006)] Mack C (2006) Field Guide to Optical Lithography. SPIE Press

[Mendes(2004)] Mendes R, Kennedy J, Neves J (2004) The fully informed particle swarm: Simpler, maybe better. IEEE Trans Evol Comp 8(3):204–210

[Selvaraja(2008)] Selvaraja S, Bogaerts W, Van Thourhout D, Baets R (2008) Fabrication of uniform photonic devices using 193 nm optical lithography in silicon-on-insulator. Proc ECIO p FrB3

[Vlasov(2004)] Vlasov YA, McNab S (2004) Losses in single-mode silicon-on-insulator strip waveguides and bends. Opt Express 12(8):1622 – 1631